



Geometric deviation evaluation for a five-axis flank milling tool path using the tool swept envelope

Yao-An Lu¹ · Cheng-Yong Wang¹ · Li Zhou²

Received: 19 June 2019 / Accepted: 3 September 2019 / Published online: 26 October 2019
© Springer-Verlag London Ltd., part of Springer Nature 2019

Abstract

The geometric deviation is a fundamental concern of five-axis flank milling tool path planning. The determination of the tool swept envelope (TSE) is a very important issue for geometric deviation evaluation because the machined surface is formed by the TSE. Envelope condition is usually utilized to calculate the swept profiles on the cutter surfaces to construct the TSE. The envelope condition presumes the velocity of any point on the tool axis trajectory surface does not vanish. However, it will vanish if the tool axis trajectory surface is not regular. If the swept profiles are still integrated directly to form the TSE when the tool axis trajectory surface is not regular, a wrong result is returned and it will affect the geometric deviation evaluation as well. Kinds of research have largely overlooked this problem. This research presents a robust TSE modeling method and an efficient geometric deviation evaluation method using the TSE. First, the two rotary axes movements are considered to define the tool axis trajectory surface. Then, based on the tool axis trajectory surface and the cutter geometry, cutter's swept profiles are determined by using the envelope theory of sphere congruence. By utilizing the proposed method to detect outlier tool positions, the TSE is decomposed into multiple surface patches according to the outlier tool positions. To deal with the tool path self-intersection issue, surface patches of the TSE and the cutting tools at the outlier tool positions are represented as triangular facets. Finally, the geometric deviation for a flank milling tool path is calculated via the discrete vector model of the design surface. Examples are given to demonstrate the validity of the proposed methods.

Keywords Geometric deviation · Tool swept envelope · Flank milling · Self-intersection tool path

1 Introduction

Five-axis flank milling is of importance to machine complex slender surfaces found mainly in aircraft structural parts, turbines, and blades. It can machine these surfaces for the advantages of larger material removal rate and eliminating necessary hand finish as compared with point milling.

Advanced algorithms of the five-axis flank milling tool path generation have been developed [1–3]. The primary goal of flank milling tool path optimization is

to reduce the geometric deviation, and many researchers have developed different geometric deviation evaluation methods. Li et al. [4] compared three different geometric deviation calculation methods for a flank milling tool path, and then they proposed two methods for the geometric deviation calculation, which are easy to be implemented. Pechard et al. [5] used a double projection method, which was an approximation method, to estimate the geometric deviation. Geometric deviation is defined as the difference between the simulation model of the machined surface and the design surface [6]. Hence, these two methods do not apply to calculate the geometric deviation accurately. Yi et al. [7] first sampled points on the design surface, and then the line segment was extended along with the positive and negative normal directions at each sampling point. The cutter sweeps across the line segments and then the geometric deviation can be determined by summing up the remaining segment length at each sampling point. The cutter motion between consecutive cutter locations needs

✉ Yao-An Lu
luyaoan@gdut.edu.cn

¹ School of Electromechanical Engineering, Guangdong University of Technology, Guangzhou 510006, China

² School of Mechatronic Engineering, Guangdong Polytechnic Normal University, Guangzhou 510635, China

to be approximated by linearly interpolating a number of intermediate cutter positions. Hence, this method is time-consuming and cost-intensive. The discrete vector method, also called point vector method, is one of the most efficient methods in NC simulation [8]. This approach approximates the design surface by a discrete set of points and vectors originating from these points. The cutting is simulated by calculating the intersection of these vectors with the cutter swept volumes. The vectors are clipped if the tool passes at that location. The discrete vector method is utilized in this research to calculate the geometric deviation.

The machined surface is the result of the cutting process where the material is removed by the cutter motion relative to the in-process workpiece, and it is part of the swept envelope generated by the cutter movements along the tool path. Only the swept profiles on the cutter surfaces contribute to the final machined surface during machining. That is, by using the tool swept envelope (TSE) to determine the geometric deviation, the cutter geometry can be simply represented by its swept profiles. Accordingly, the processing time to calculate the geometric deviation can be reduced significantly. Zhu et al. [9] proposed the point-to-surface distance function to compute the geometric deviation between the swept envelope and a point on the design surface without constructing the TSE itself. However, an initial solution is required to solve the nonlinear equations by an iterative approach, and it is not an easy task to get a good initial solution. Moreover, this method still calculates the minimum distance between the swept envelope and a point locating on the portion of the design surface which is not cut by the cutter. Hence, it cannot calculate the geometric deviation accurately in this case.

Several mathematical algorithms have been developed to construct the TSE, such as envelope theory, sweep-envelope differential equation, and singularity theory. The envelope theory is used widely. Usually, a discretization for the tool path is first introduced, and subsequently, the swept profiles on the cutter surfaces are connected for constructing the TSE. Du et al. [10] formulated the swept profiles for cutters undergoing five-axis motions based on the moving frame and rigid body motions. Gong et al. [11] proposed two closed-form solutions for calculating the TSE of a generic tool directly from the cutter location (CL) data based on the moving frame method. Based on the tangency condition, Zhu et al. [12] derived a closed-form solution of the swept envelope of a general rotary cutter moving along a general tool path. Aras [13] presented an efficient parametric approach of determining the shape of the envelope surface formed by a generalized cutter

following the five-axis tool path. Lee et al. [14] presented an approach to find the swept volume of a tool undergoing a five-axis movement using the Gauss map. However, this approach is only applicable to the cutters which have the convex hull property on the cutting part. Later, Zhu et al. [15] also derived the necessary and sufficient conditions for tangent continuity of two adjacent TSEs, and it was applied to generate flank milling tool paths. Li et al. [16] integrated the cutter runout effect into TSE modeling. Zhou et al. [6] first proposed an approach to calculate the envelope surface and then evaluated the geometric deviation using the TSE.

The more difficult problem of TSE generation is self-penetration or self-intersection which arises when the instantaneous center of rotation of the moving tool is located inside the tool body [17]. When self-penetration phenomena occur, a portion of the TSE penetrates itself and then it cannot get a topologically consistent swept envelope without extra geometrical treatment. Self-intersection tool paths are quite normal in five-axis milling. It requires special processing to handle the self-intersection problem in order to evaluate the geometric deviation. However, the theme “self-intersection of TSE” has been neglected or skipped in most researches on the TSE modeling and the geometric deviation evaluation. Blackmore et al. [18] established an efficient method of both local and global trimming of the swept volume. However, trimming is time-consuming. Lee et al. [17] first presented the necessary condition of the self-penetration of a cutter at five-axis movements, and then they described a method of trimming the invalid facets interior to the swept volume for machining simulation. Machchhar et al. [19] first developed a system of algebraic constraints to model the TSE, and then they utilized a dixel-based algorithm to compute the swept volume of cutters for machining simulation, solving the self-intersection problem in the envelope construction.

Many TSE modeling methods utilize the envelope condition, which is the instantaneous velocity at a surface point of the generator is perpendicular to the surface normal at this point, to determine grazing points. According to [11], the envelope condition for a surface of revolution, i.e., rotary cutter surface, is $\mathbf{v}(l, t) \cdot \mathbf{n}(\theta, l, t) = 0$, where l and t are the two parameters of the tool axis trajectory surface, and θ denotes the oriented angle around the tool axis. $\mathbf{n}(\theta, l, t)$ is the normal of the surface of revolution at the grazing point, and $\mathbf{v}(l, t)$ denotes the velocity of the point lying on the tool axis trajectory surface at parameter (l, t) . The assumption of this condition is that the boundary of the rotary cutter is a regular surface [20] and $\mathbf{v}(l, t)$ does not vanish. However, $\mathbf{v}(l, t)$ may vanish when the tool axis trajectory surface is not regular. Considering a

parametric surface $S(u, v)$, and S_u and S_v denote the partial differentiation with respect to u and v respectively. A regular (ordinary) point p on a parametric surface is defined as a point where $S_u \times S_v \neq 0$. A point which is not a regular point is called a singular point. The condition $S_u \times S_v \neq 0$ requires that the vectors S_u and S_v at point p do not vanish and have different directions. A surface is regular if it is regular at all points $p \in S$. Types of related research on the TSE modeling estimate the case when the tool axis trajectory surface is not regular.

A two-parameter family of spheres would be generated if a rotary cutter undergoes a one-parameter spatial motion [1]. Compared to other TSE modeling methods in milling, the theory of two-parameter families of spheres provides a simpler calculation [9]. Hence, it is utilized to generate the TSE of a flank milling tool path in this research. In this research, a cutter location is an outlier cutter location when the unregular points on the tool axis trajectory surface belong to the tool axis of this cutter location. The main contributions of this research are as follows: (1) a method of detecting whether the tool axis trajectory surface is regular, (2) an approach for decomposing the TSE of a flank milling tool path into multiple surface patches according to the outlier cutter locations, and (3) the surface patches of the TSE and the tool surfaces at the outlier tool positions are tessellated with triangles, so that the proposed geometric deviation evaluation method can handle all cases of the tool paths in a consistent way.

The remainder of this paper is organized as follows. In Sect. 2, the preliminaries for the TSE generation are presented. The method of detecting whether the tool axis trajectory surface is regular is described in Sect. 3, as well as the method of decomposing the TSE into multiple surface patches. Method of the geometric deviation evaluation via the discrete vector model of the design surface is introduced in Sect. 4. Numerical examples are presented in Sect. 5, and conclusions are given in Sect. 6.

2 Preliminaries

Before we give the detailed calculation process, some preparatory work should be done first.

2.1 Tool path representation with rotary axis movements

A tool axis trajectory surface can be defined by using the two curves expressed in the part coordinate system, which define the locus of the tool tip locations and the locus of a second point belonging to the tool axis respectively [21]. In order to determine the swept profiles based on the true rotary axes movements of the utilized machine tool, we use three B-spline curves to define a five-axis milling path. The three spline curves are $P(u)$ for the cutter reference point trajectory

in the part coordinate system (PCS) and the other two splines represent the displacements of the two rotary axes of the five-axis machine tool along the tool path. Therefore, the tool axis trajectory surface of a milling tool path can be expressed as

$$S(u, v) = P(u) + v \cdot H \cdot O(u) \tag{1}$$

where H is the axial height of the cutting part of a cutter, $v \in [0, 1]$, and $O(u)$ denotes the unit tool orientation. $O(u)$ is represented with the two rotary axis displacements. The inverse kinematics transformation (IKT) of the particular five-axis machine tool can convert the unit tool orientation into the two rotary axes displacements. Details can be found in [22].

2.2 Envelope theory of sphere congruence

A two-parameter family of spheres would be generated if the cutter undergoes a one-parameter spatial motion. The TSE is identically the envelope surface of this two-parameter family of spheres [1]. The fundamental theory of sphere congruence is briefly introduced in this section, and details can be referred to [9]. The TSE $X(u, v)$ generated by a cutter moving along a tool path can be formulated as

$$X(u, v) = S(u, v) + r(u, v)n(u, v) \tag{2}$$

where $S(u, v)$ denote the tool axis trajectory surface as expressed in Eq. (1), $n(u, v)$ is the unit normal vector of the envelope, and $r(u, v)$ is the radius of any sphere in the family. It is worth noting that the domain $[v_0, v_1]$ of the surface parameter v in Eq. (2) is not $[0, 1]$, and it is decided according to the rotary cutter geometry. More details can be referred to [9]. Two tangent vectors of the envelope surface can be obtained by calculating the partial derivatives of $X(u, v)$.

$$X_u = S_u + r n_u, \quad X_v = S_v + r_v n + r n_v \tag{3}$$

Without loss of generality, here we take a BC-type spindle-table machine tool as an example. Let $C_B(u)$ and $C_C(u)$ denote the displacement curves of the two rotary axes, respectively. Suppose the two rotary axes displacements are θ_C and θ_B , respectively, at the surface parameter u_0 . The relationship between the rotary axis position and the tool orientation for a BC-type spindle-table machine tool is expressed as

$$\begin{aligned} i(u_0) &= \cos(\theta_C)\sin(\theta_B), \quad j(u_0) = -\sin(\theta_C)\sin(\theta_B), \\ k(u_0) &= \cos(\theta_B) \end{aligned} \tag{4}$$

Then, $O(u_0) = [i(u_0) \ j(u_0) \ k(u_0)]^T$. Hence, $S_u = P_u + v \cdot H \cdot \frac{dO(u)}{du}$, $S_v = H \cdot O(u)$ according to Eq. (1). Let $n^s(u, v)$

denotes the unit normal vector of $S(u, v)$, and the vector n can be expressed in terms of the Gauss frame of $S(u, v)$ as

$$n = \alpha S_u + \beta S_v + \gamma n^s \tag{5}$$

The coefficients in Eq. (5) can be obtained as

$$\alpha = -A_{12}r_v, \quad \beta = -A_{22}r_v, \quad \gamma = \pm \sqrt{1-r_v^2 A_{22}} \tag{6}$$

where $\begin{bmatrix} A_{11} & A_{12} \\ A_{21} & A_{22} \end{bmatrix} = \begin{bmatrix} g_{11} & g_{12} \\ g_{21} & g_{22} \end{bmatrix}^{-1}$, and $g_{11} = S_u \cdot S_u$, $g_{12} = g_{21} = S_u \cdot S_v$, $g_{22} = S_v \cdot S_v$. It should note that it is singularity when $1-r_v^2 A_{22} < 0$, and no grazing point can be acquired. Two TSEs are formed by the cutter movements along the tool path. The envelope surface that generates the machined surface is called the effective envelope surface (S_{EE}), and the other envelope surface is called the auxiliary envelope surface (S_{AE}).

2.3 Tool swept envelope modeling

Self-intersecting tool paths are quite normal in five-axis milling, and the TSEs modeling of the self-intersecting tool path requires special processing to handle the topological problems. Here, triangular facets are employed to represent the TSEs. In order to represent the TSEs as triangular facet models, defining vertices for each facet are required. To define these vertices, a set of uniform points needs to be generated. Hence, each swept profile on the cutter surface is tessellated into points and the number of the points is identical. The points are generated in sequential order, and then each facet can be constructed sequentially. Finally, the TSEs are modeled as triangular facets.

3 Method of decomposing TSE into surface patches

The assumption of the envelope theory is that the trajectory of the cutting tool is a regular surface, which means that it has no sharp points or edges. However, kinds of research on TSE modeling have not handled the case when the tool axis trajectory surface is not a regular surface.

Considering the tool axis trajectory surface $S(u, v)$ of a flank milling path as expressed in Eq. (1) and the domain of the surface parameter v is $[v_0, v_1]$. S_u and S_v denote the partial differentiation with respect to u and v . $S_v(u, v) = H \cdot O(u)$ is the tool orientation of the cutter at surface parameter u , and it does not vanish in any case. However, $S_u(u, v) = P_u(u) + v \cdot H \cdot O_u(u)$ may has zero or very small magnitude. For a given parameter u_0 , $S(u_0, v_i)(v_i \in [v_0, v_1])$ is a point on the segment

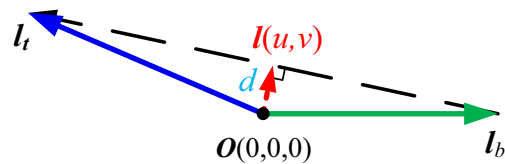


Fig. 1 Diagram of $I(u, v)$

which starts from point $P(u_0)$ and orientation is tool axis $O(u_0)$. The partial differentiation of $S(u, v)$ with respect to parameter u at the parametric coordinate (u_0, v_i) can be determined as

$$I(u_0, v_i) = I_b(u_0) \cdot \left(1 - \frac{v_i - v_0}{v_1 - v_0}\right) + I_t(u_0) \cdot \frac{v_i - v_0}{v_1 - v_0} \tag{7}$$

where $I_b(u_0) = P_u(u_0) + v_0 \cdot H \cdot O_u(u_0)$ and $I_t(u_0) = P_u(u_0) + v_1 \cdot H \cdot O_u(u_0)$. The subscript u represents the corresponding partial derivative. I_t and I_b are the partial differentiation of $S(u, v)$ with respect to u at $v = v_0$ and $v = v_1$ respectively. It can be seen from Eq. (7) that $I(u, v)$ varies linearly with parameter v .

The following method can be used to detect whether $I(u, v)$ vanishes. Let point $A = I_b$ and $B = I_t$, then the minimum distance d between the origin point $O(0, 0, 0)$ to the segment AB can be calculated, as illustrated in Fig. 1. If $d < \epsilon$ where ϵ is a specified small value, it means $I(u, v)$ vanishes, and the associated cutter location at the parameter u is an outlier cutter location. The number of discretization intervals within the domain $[u_s, u_e]$ of parameter u of the tool path should be large enough, so that it can find all the potential outlier cutter locations.

Once outlier cutter locations are detected, the swept profiles have to be decomposed according to the outlier tool positions, and then forming the surface patches of the TSEs. Swept profiles on the cutter surfaces need to be determined first to construct the TSE. Hence, let the set $U_1 = \{u_i; i = 0, 1, \dots, n_1\}$ denote the parameters of the sampled cutter location data along the tool path. Let $U_2 = \{t_i; i = 0, 1, \dots, n_2\}$ denote the parameter sequence of the outlier tool positions along the tool path. Let t_{j-1} and t_j be the $(j-1)$ th and j th elements in U_2 . Finding k and m that satisfy $u_k < t_{j-1} < u_{k+1}$ and $u_m < t_j < u_{m+1}$, respectively, then the swept profiles on the cutter surfaces between the $(k+1)$ th and m th tool positions along the tool path are connected to construct the surface patches of the TSEs. It should be mentioned that it cannot form a surface patch if $m = k + 1$, because there is only one swept profile. Besides, if $m = k$, it means t_{j-1} and t_j locate at the same parameter interval, and a surface patch cannot be formed either. Repeating the above procedures for U_2 of all the parameters of the outlier tool positions, we finally can get the surface patches which are a portion of the TSEs. Algorithm 1 describes the method of decomposing the TSEs into multiple surface patches.

Algorithm 1 method of decomposing the TSEs into surface patchesInput: the sets $U_1 = \{u_i; i = 0, 1, \dots, n_1\}$ and $U_2 = \{t_i; i = 0, 1, \dots, n_2\}$

Output: multiple surface patches

Main routine

- (1) For $j = 0, 1, \dots, n_2$
- (2) if $j = 0$
- (3) **Find** k that satisfies $u_k < t_j < u_{k+1}$
- (4) **Form** surface patches using the intermediate swept profiles between the first and k th tool positions
- (5) else if $j \neq n_2$
- (6) **Find** k and m that satisfy $u_k < t_{j-1} < u_{k+1}$ and $u_m < t_j < u_{m+1}$
- (7) if $m = k+1$ or $m = k$
- (8) continue
- (9) else
- (10) **Form** surface patches using the intermediate swept profiles between the $(k+1)$ th and m th tool positions
- (11) end if
- (12) else
- (13) **Find** k that satisfies $u_k < t_j < u_{k+1}$
- (14) **Form** surface patches using the intermediate swept profiles between the k th and last tool positions
- (15) end if
- (16) end for

4 Geometric deviation evaluation

The discrete vector model (DVM) represents the workpiece as a set of direction vectors emanating from a grid on the workpiece surface, where the directions are the normal vectors at the corresponding surface points, and the length L of each vector represents the depth of the workpiece geometry. The discrete vectors are updated as the cutter sweeps through different regions of the grid, capturing the new heights of the direction vectors. A positive value of L at a position denotes that there remains material to be cut. On the other hand, overcut or gouging occurs if L is negative [23]. The diagram of the DVM is illustrated in Fig. 2.

Grazing points on the cutter surfaces are first determined by using Eq. (2), and then we can model the TSEs as triangular meshes for the geometric deviation evaluation. Moreover, the triangular facet model is also utilized to represent the cutter surfaces at all the outlier cutter locations.

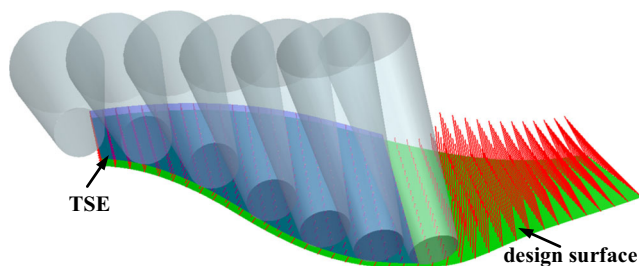


Fig. 2 Diagram of the discrete vector method

4.1 Localization of facets

The most time-consuming and frequent process in the geometric deviation evaluation is computing the intersections between TSEs, cutter surfaces, and discrete vectors of the workpiece model. Therefore, it is necessary to locate the facets affected by a given discrete vector. We can find the affected vertices of the facets first by using the octree algorithm in [24] and then acquire the associated facets.

4.2 Facet-segment intersection

Let the facets of the TSEs be represented as $F = \{f_i, i = 0, 1, \dots, m\}$. Also, let a set of discrete vectors of the DVM be $V = \{v_k, k = 0, 1, \dots, n\} = \{(c, N, L)_k\}$, where c is a point lying on the design surface, N is the unit normal vector at c , and L_k is the current length of v_k measured from c . Now the basic function is to find out whether the k th discrete vector v_k intersects the i th triangle f_i and the corresponding intersection point if they have intersections. Note that v_k is geometrically identical to a three-dimensional line segment whose parametric equation is expressed as $p(t) = c_k + tN_k, \lambda \leq t \leq L_k$, where λ is some negative value smaller than L_k . Note that λ is a given fixed value only determining the negative endpoint of v_k . TSEs with self-penetration can have facets which are located within itself because a portion of the swept profiles is immersed into the tool body. Hence, the segment $p(t)$ may

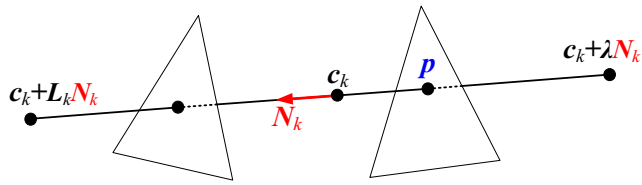


Fig. 3 Diagram of the facet-segment intersection

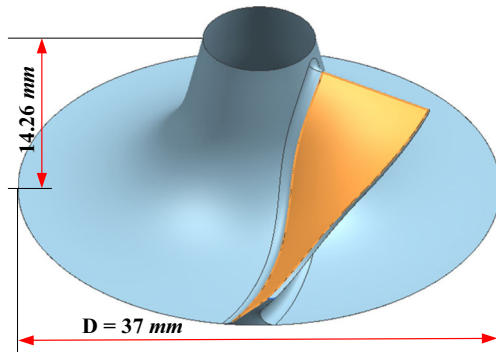


Fig. 4 The blade surface and the impeller model

Fig. 5 Evolutions of the two rotary axes along the tool path

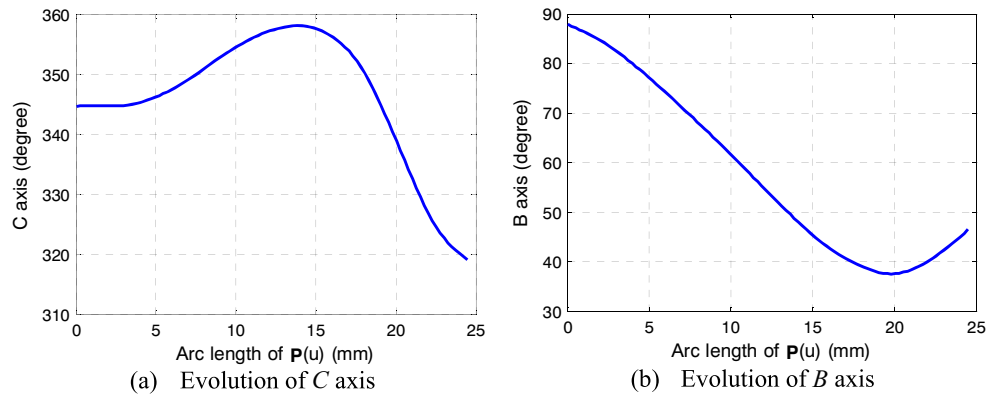
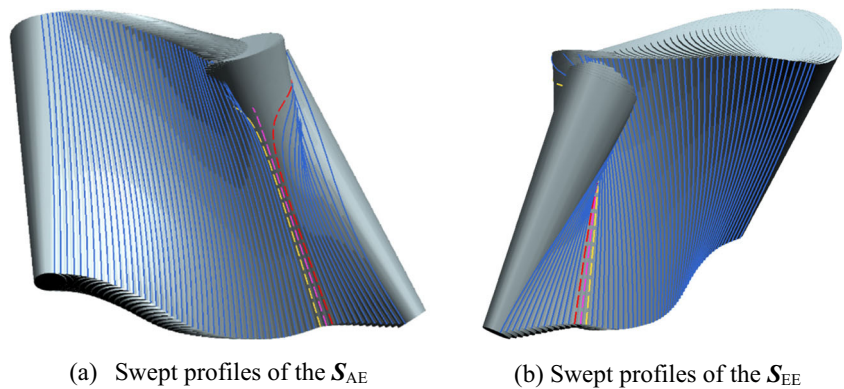


Fig. 6 Swept profiles represented on the cutter surfaces



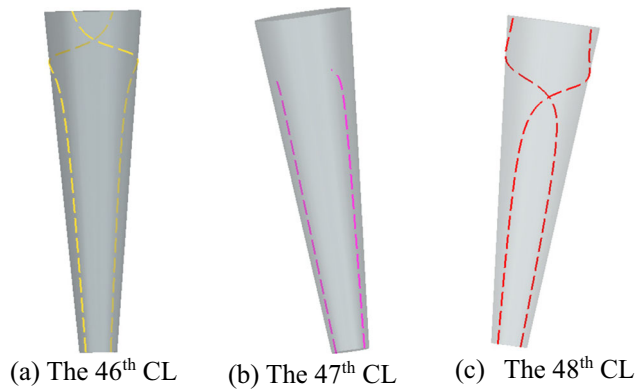


Fig. 7 Swept profiles on the cutter surfaces at the three tool positions

intersect multiple triangles, as presented in Fig. 3. If intersections occur at $t = \omega_j (j = 0, 1, \dots, n_0)$ between the triangles and the segment $\mathbf{p}(t)$ with $\lambda < \omega_j < L_k$, the final selected intersection point is $\mathbf{p} = \mathbf{c}_k + \omega_{\min} \mathbf{N}_k$, and $\omega_{\min} = \min \{\omega_j; j = 0, 1, \dots, n_0\}$. Then, L_k is to be replaced with ω_{\min} to incorporate this cut. Repeating this test for \mathbf{V} , we finally can get the geometric deviation.

5 Numerical simulations

The proposed method has been implemented by using the C++ language with the 3D geometric modeler ACIS. This section illustrates two verifications of the five-axis flank milling tool path geometric deviation evaluation for sculptured surfaces using the proposed approach. A spindle-table BC-type five-axis machine tool is utilized. The relationship

between the rotary axis position and the tool orientation for this machine tool is expressed in Eq. (4). The strokes of the two rotary axes are $B \in [-10^\circ, 120^\circ]$, $C \in [0^\circ, 360^\circ]$. The degree of B-spline curve is 5, and $\varepsilon = 0.1$.

5.1 Case study 1

The blade surface utilized in this case study is illustrated in Fig. 4. A conical cutter with parameter $r = 1 \text{ mm}$, $\varphi = 5^\circ$, $H = 18 \text{ mm}$ is used in this case study. Twenty-five cutter locations are first determined using Chiou’s method [25]. After acquiring the cutter location data, the corresponding displacements of the two rotary axes for each cutter location data can be calculated with the IKT of the machine tool. For a given tool orientation, there are multiple possible solutions for B and C axis displacements. In this case study, the Dijkstra’s shortest path algorithm is employed to choose the appropriate rotary axes solutions among the candidates. After that, the cutter reference point trajectory and the displacement curves of the two rotary axes along the tool path can be acquired by using the interpolation method described in [21, 22]. The evolutions of the two rotary axes B and C during the path are presented in Fig. 5.

After the interpolation, the surface parameter domain of this five-axis tool path can be determined, and $v_0 = r \tan(\varphi) / H$, $v_1 = (H + \tan(\varphi) \cdot (H \tan(\varphi) + r)) / H$. Accordingly, it is $(u, v) \in [0, 24.49] \times [0.0049, 1.0125]$ in this case study. Sixty cutter location data are sampled along the tool path to calculate the swept profiles. Two swept profiles on the cutter surface at each tool position along the tool path are determined. The swept profiles and the associated cutter models at the

Fig. 8 The TSEs

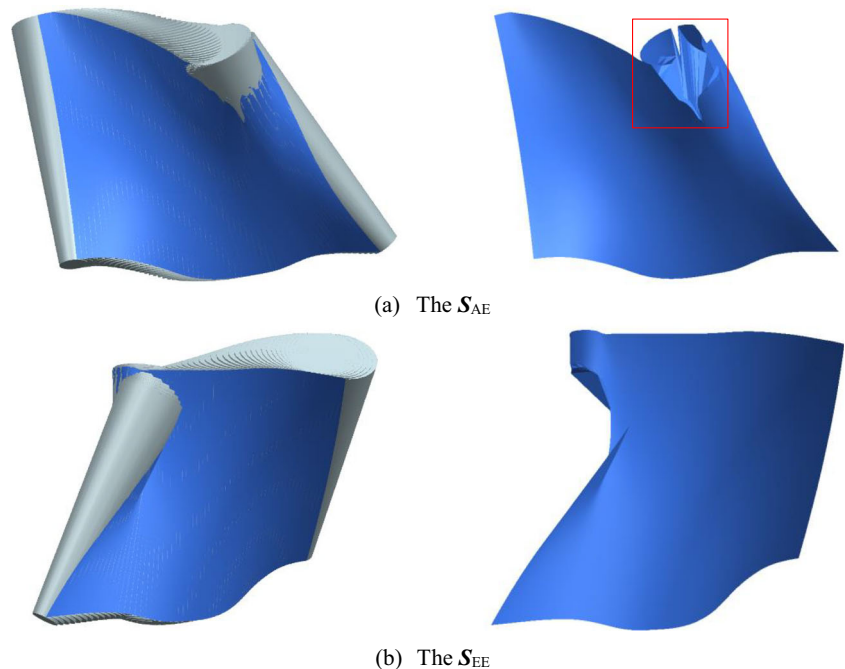
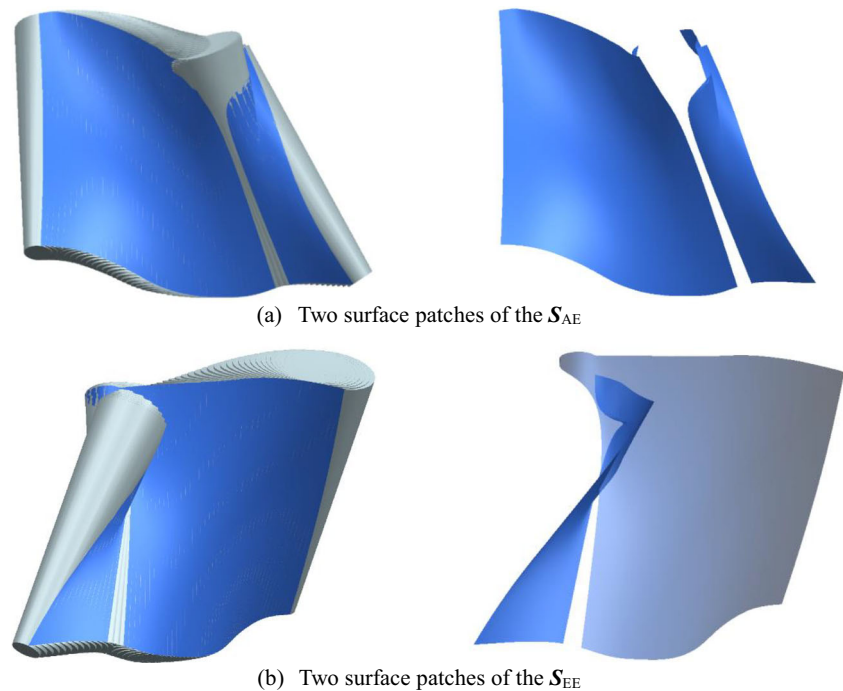


Fig. 9 Surface patches of the TSEs



discrete parameters are illustrated in Fig. 6. As can be seen in Fig. 6, self-intersection occurs, and the shape of the neighboring swept profiles represented with dashed vary greatly. The swept profiles on these three cutter surfaces are given in Fig. 7, and the swept profiles wind the tool body as presented in Fig. 7a and Fig. 7c. It raises a problem with the existence of grazing points at one of the tool positions, as illustrated in Fig. 7b. In other words, no corresponding grazing points exist in some ranges of v . If these neighboring swept profiles are linearly interpolated to construct the TSEs, as shown in Fig. 8, it is not correct.

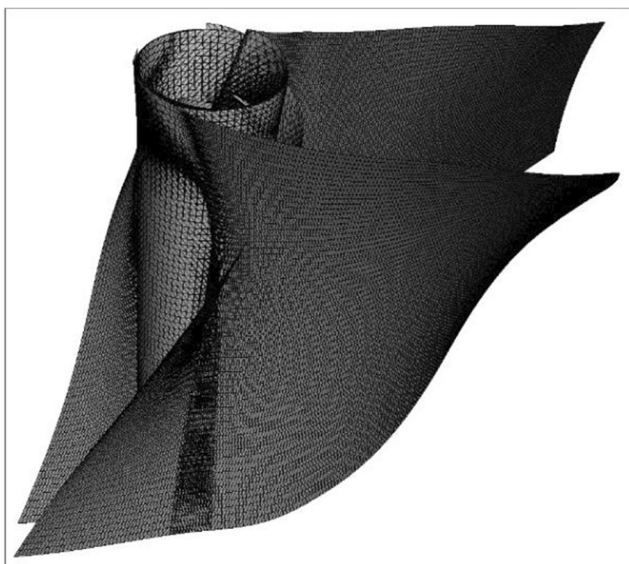


Fig. 10 Triangular facets of the surface patches and the cutter surfaces

When it requires to calculate the geometric deviation of a tool path which has outlier cutter locations and is self-intersection, the TSEs have to be decomposed into multiple surface patches, and triangle-mesh-based cutter models are utilized to model the cutter at all the outlier cutter locations along the tool path as a set of connected triangles. The triangle size is user-selected. However, the small triangle size leads to numerous triangles, which slows down the involved calculations. So, in practice, the triangle size is selected to balance the modeling accuracy and calculation time. The number of sampled cutter locations n_1 , which is described in Sect. 3, should be chosen such that the distance between swept profiles is about the selected triangle size of the cutter model. Therefore, 200 cutter locations are sampled along the tool path and the swept profiles are also calculated.

A large number is required for discretization intervals to find all the potential outlier cutter locations along the tool path. Hence, the domain of the cutter reference point trajectory $P(u)$, which is identical to the domain of the surface parameter u of the tool axis trajectory surface, is tessellated into 10,000 points and the method described in Sect. 3 is utilized to detect whether there exist outlier cutter locations. It is founded that the cutter locations, whose cutter location point's u -parameter are within the range [18.230, 19.243], are outlier cutter locations. Hence, the cutter location, which among the 200 sampled cutter locations and whose u -parameter of the cutter location point belongs to the set {18.337, 18.460, 18.583, 18.706, 18.829, 18.952, 19.075, 19.198}, is an outlier cutter location. The TSEs are then decomposed into surface patches according to the outlier cutter positions. The surface patches of the TSEs are shown in Fig. 9.

To evaluate the geometric deviation for the generated tool path, 100×40 points are sampled on the blade surface. The allowance left is 2 mm. The triangular facets of the surface patches of the TSEs and the cutter surfaces at the outlier tool positions, as shown in Fig. 10, are utilized to calculate the intersection points with the discrete vectors of the workpiece surface, acquiring the geometric deviation. The distribution of the geometric deviation is presented in Fig. 11.

5.2 Case study 2

The *S*-shaped surface utilized in this case study is illustrated in Fig. 12. A conical cutter with parameter $r=4$ mm, $\varphi=3^\circ$, $H=25$ mm is used in this case study. Eighty cutter locations are first determined using Chiou's method [25], and the evolutions of the two rotary axes *B* and *C* along the tool path are presented in Fig. 13. It is worth mentioning that the solutions of *B* and *C* axis are not chosen by utilizing the Dijkstra's shortest path algorithm in this case study. The way to select the rotary axes displacement solutions in this case study is described as follows. The following displacements for the *B* and *C* axes are determined according to the previous *B* and *C* axis displacements by selecting the solution which causes the shortest rotational movement. Large movements can be found in the evolutions of the two rotary axes because of the stroke limit of the *B* axis, as illustrated in Fig. 13. The two rotary axes movements result in the tool axis trajectory surface is not regular, which is appropriate to verify the proposed method.

Fig. 11 Distribution of the geometric deviation

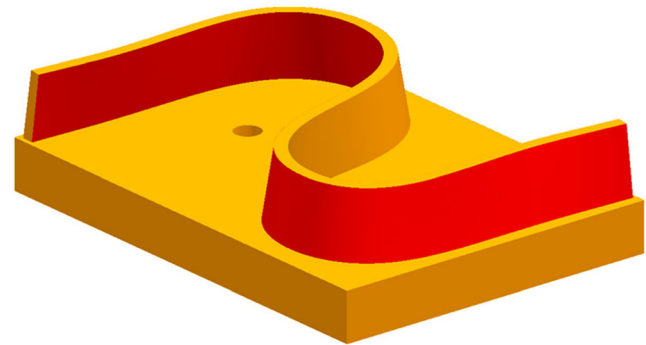
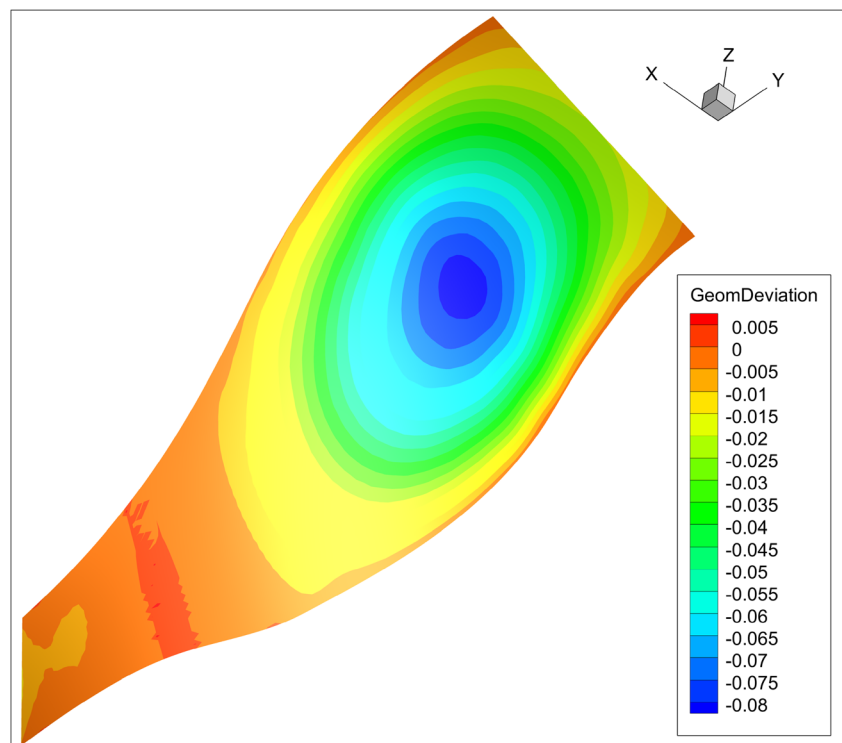


Fig. 12 The *S*-shaped part

The domain of the cutter reference point trajectory is tessellated into 50,000 points and then the proposed method is employed to detect whether there exist outlier cutter locations. It is found that outlier cutter locations exist. To form the TSEs, 1200 cutter locations are sampled along the tool path to calculate the swept profiles. The TSEs are decomposed into surface patches according to the outlier cutter positions. The surface patches of the TSEs are shown in Fig. 14.

Employing the triangular facets to represent the surface patches and the cutter models at the outlier tool positions, the geometric deviation is calculated. The allowance left is 2 mm. 1000×60 points are sampled on the *S* surface, and the distribution of the geometric deviation is presented in Fig. 15.

Fig. 13 Evolutions of the two rotary axes along the tool path

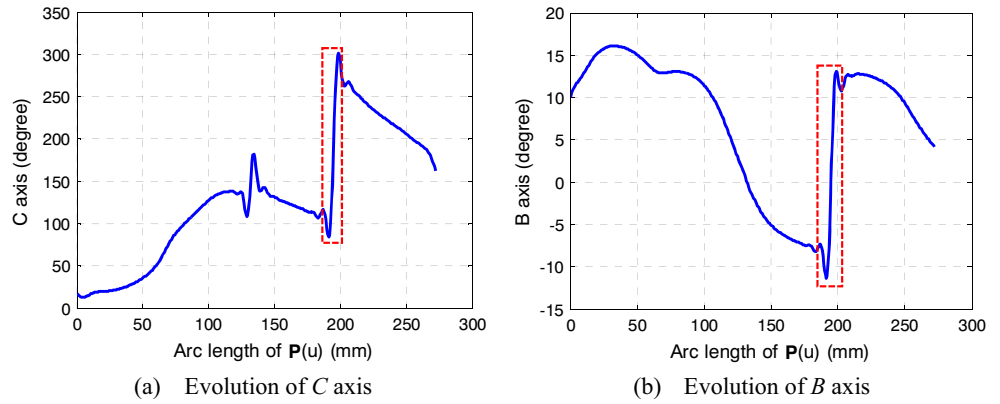


Fig. 14 Surface patches of the TSEs

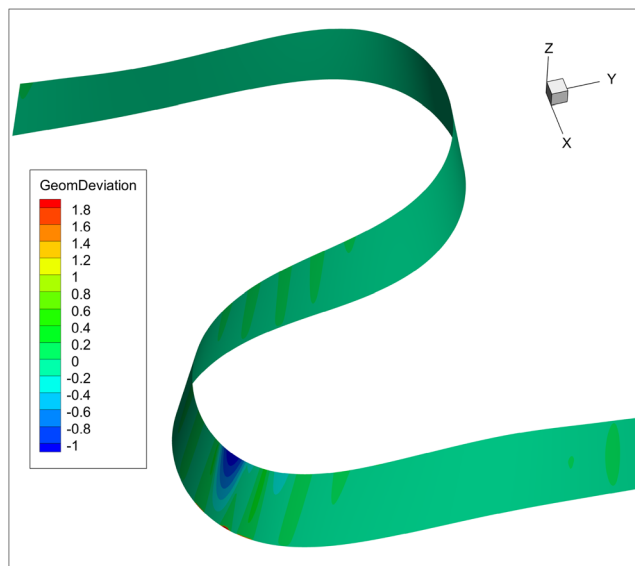
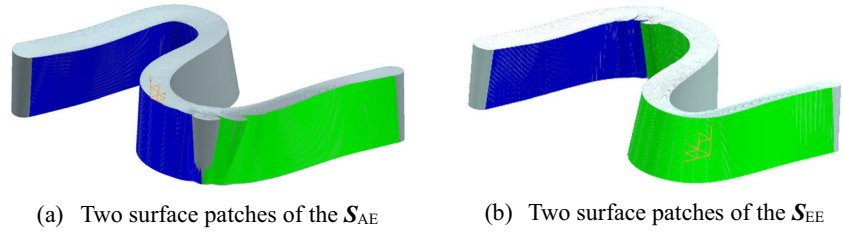


Fig. 15 Distribution of the geometric deviation

6 Conclusions

The velocity of any point on the tool axis trajectory surface may vanish if the tool axis trajectory surface is not regular, and then outlier cutter locations exist. This research proposes a robust TSE modeling method. The outlier tool positions are first detected utilizing the proposed method, and then the TSEs are decomposed into multiple surface patches according to the outlier tool positions if they exist. The surface patches of the TSEs are modeled as triangle meshes to handle the topological problem of TSE modeling for self-intersection tool paths. The cutter surface at the outlier tool positions are also represented as triangular facets, and the discrete vector model of the design surface is employed to calculate the geometric deviation. The effectiveness of our method is demonstrated on two simulation examples.

Acknowledgments This work was supported by the Science and Technology Planning Project of Guangdong Province (Grant Number 2017B090913006), the National Natural Science Foundation of China (Grant Number 51805094), and the China Postdoctoral Science Foundation (Grant Number 2018M633009).

References

- Zhu LM, Zheng G, Ding H, Xiong YL (2010) Global optimization of tool path for five-axis flank milling with a conical cutter. *Comput Aided Des* 42(10):903–910
- Huang ND, Bi QZ, Wang YH, Sun C (2014) 5-Axis adaptive flank milling of flexible thin-walled parts based on the on-machine measurement. *Int J Mach Tool Manu* 84:1–8
- Calleja A, Bo PB, González H, Bartoň M, López de Lacalle LN (2018) Highly accurate 5-axis flank CNC machining with conical tools. *Int J Adv Manuf Technol* 97(5–8):1605–1615
- Li C, Mann S, Bedi S (2005) Error measurements for flank milling. *Comput Aided Des* 37(14):1459–1468
- Pechard PY, Tournier C, Lartigue C, Lugarini JP (2009) Geometrical deviations versus smoothness in 5-axis high-speed flank milling. *Int J Mach Tool Manu* 49(6):454–461
- Zhou YS, Chen ZZC, Yang XJ (2015) An accurate, efficient envelope approach to modeling the geometric deviation of the machined surface for a specific five-axis CNC machine tool. *Int J Mach Tool Manu* 95:67–77
- Yi J, Chu CH, Kuo CL, Li XY, Gao L (2018) Optimized tool path planning for five-axis flank milling of ruled surfaces using geometric decomposition strategy and multi-population harmony search algorithm. *Appl Soft Comput* 73:547–561
- Sullivan A, Erdim H, Perry RN, Frisken SF (2012) High accuracy NC milling simulation using composite adaptively sampled distance fields. *Comput Aided Des* 44(6):522–536
- Zhu LM, Zhang XM, Zheng G, Ding H (2009) Analytical expression of the swept surface of a rotary cutter using the envelope theory of sphere congruence. *J Manuf Sci Eng* 131(4):041017
- Weinert K, Du S, Damm P, Stautner M (2004) Swept volume generation for the simulation of machining processes. *Int J Mach Tool Manu* 44(6):617–628
- Gong H, Wang N (2009) Analytical calculation of the envelope surface for generic milling tools directly from CL-data based on the moving frame method. *Comput Aided Des* 41(11):848–855
- Zhu LM, Zheng G, Ding H (2009) Formulating the swept envelope of rotary cutter undergoing general spatial motion for multi-axis NC machining. *Int J Mach Tool Manu* 49(2):199–202
- Aras E (2009) Generating cutter swept envelopes in five-axis milling by two-parameter families of spheres. *Comput Aided Des* 41(2):95–105
- Lee SW, Nestler A (2011) Complete swept volume generation—part I: swept volume of a piecewise C1-continuous cutter at five-axis milling via Gauss map. *Comput Aided Des* 43(4):427–441
- Zhu LM, Lu YA (2015) Geometric conditions for tangent continuity of swept tool envelopes with application to multi-pass flank milling. *Comput Aided Des* 59:43–49
- Li ZL, Zhu LM (2014) Envelope surface modeling and tool path optimization for five-axis flank milling considering cutter runout. *J Manuf Sci Eng* 136(4):041021
- Lee SW, Nestler A (2011) Complete swept volume generation—part II: NC simulation of self-penetration via comprehensive analysis of envelope profiles. *Comput Aided Des* 43(4):442–456
- Blackmore D, Samulyak R, Leu MC (1999) Trimming swept volumes. *Comput Aided Des* 31(3):215–223
- Machchhar J, Plakhotnik D, Elber G (2017) Precise algebraic-based swept volumes for arbitrary free-form shaped tools towards multi-axis CNC machining verification. *Comput Aided Des* 90:48–58
- Wang WP, Wang KK (1986) Geometric modeling for swept volume of moving solids. *Comput Graph Appl* 6(12):8–17
- Langeron JM, Duc E, Lartigue C, Bourdet P (2004) A new format for 5-axis tool path computation, using B-spline curves. *Comput Aided Des* 36(12):1219–1229
- Lu YA, Wang CY, Zhou L, Sui JB, Zheng LJ (2019) Smooth flank milling tool path generation for blade surfaces considering geometric constraints. *Int J Adv Manuf Technol* 103(5):1911–1923
- Park JW, Shin YH, Chung YC (2005) Hybrid cutting simulation via discrete vector model. *Comput Aided Des* 37(4):419–430
- Behley J, Steinhage V, Cremers AB (2015) Efficient radius neighbor search in three-dimensional point clouds. Paper presented at the 2015 IEEE International Conference on Robotics and Automation (ICRA)
- Chiou JCJ (2004) Accurate tool position for five-axis ruled surface machining by swept envelope approach. *Comput Aided Des* 36(10):967–974

Publisher's note Springer Nature remains neutral with regard to jurisdictional claims in published maps and institutional affiliations.